

Invariant Description of Rigid Body Motion Trajectories

Joris De Schutter¹

Department of Mechanical Engineering,
Katholieke Universiteit Leuven,
Celestijnenlaan 300,
P.O. Box 02420,
3001 Leuven-Heverlee, Belgium
e-mail: joris.deschutter@mech.kuleuven.be

This paper presents a minimal invariant coordinate-free description of rigid body motion trajectories. Based on a motion model for the instantaneous screw axis, a time-based coordinate-free description consisting of six scalar functions of time is defined. Analytical formulas are presented to obtain these functions from the pose or twist coordinates of a motion trajectory. The time-based functions are then stripped from their temporal information yielding five independent geometric functions together with a scalar motion profile. The geometric functions are shown to be invariant with respect to time scale, linear and angular scale, motion profile, reference frame, and reference point on the rigid body used to express the translational components of the motion. An algorithm is given to reconstruct a coordinate representation of a motion trajectory from its coordinate-free description. A numerical example illustrates the validity of the approach.

[DOI: 10.1115/1.4000524]

Nomenclature

$\{a\}$ =reference frame.

a_cT = homogeneous transformation matrix representing the pose of frame $\{a\}$ with respect to frame $\{c\}$.

${}^a_c\mathbf{t}^b$ =twist of frame $\{a\}$ with respect to frame $\{c\}$, with $\mathbf{t}=(\boldsymbol{\omega}^T \mathbf{v}^T)^T$; b represents the reference point to express the translational velocity \mathbf{v} ; and $\{d\}$ represents the frame in which the coordinates of $\boldsymbol{\omega}$ and \mathbf{v} are expressed. For convenience, reference point b may formally be replaced by a frame; in that case the reference point to express the translational velocity corresponds to the origin of that frame. When obvious from the context, the subscripts and superscripts are omitted. When b corresponds to the origin of $\{d\}$, \mathbf{t} is known as a *screw twist*.

i_fS =screw transformation matrix which transforms a screw twist from an initial reference frame $\{i\}$ to another reference frame $\{f\}$, with:

$${}^i_fS = \begin{pmatrix} {}^i_f\mathbf{R} & \mathbf{0}_3 \\ [{}^i_f\mathbf{p}^f] {}^i_f\mathbf{R} & {}^i_f\mathbf{R} \end{pmatrix} \quad (1)$$

a_cR =rotation transformation matrix from $\{a\}$ to $\{c\}$.

${}^c_a\mathbf{p}$ =vector from the origin of $\{c\}$ to the origin of $\{a\}$, expressed in $\{c\}$.

$[p]$ =skew-symmetric matrix which corresponds to the vector product with vector p

$$[p] = \begin{pmatrix} 0 & -p_z & p_y \\ p_z & 0 & -p_x \\ -p_y & p_x & 0 \end{pmatrix} \quad (2)$$

\bar{q} =dimensionless or normalized quantity q .

¹Corresponding author.

Contributed by the Mechanisms and Robotics Committee of ASME for publication in the JOURNAL OF MECHANISMS AND ROBOTICS. Manuscript received December 27, 2008; final manuscript received July 18, 2009; published online November 19, 2009. Editor: J. Michael McCarthy.

1 Introduction

In robotics, especially cognitive robotics, there is a need to represent human or robot motion in a way that facilitates recognition, classification, and characterization of an executed motion, as well as model based generation of a motion that is adapted to a specific task and task environment. Examples include recognizing human motions or gestures [1–3], recognizing robot motions (for example in robot competitions), estimating human motion intention during collaborative human-robot manipulation [4], extracting a robot trajectory model from multiple human demonstrations [5,6], making a robot move in a humanlike way, and building a library of task primitives. At present no representation, which facilitates these tasks exists, even for the three-dimensional (3D)-motion of a single rigid body involving simultaneous translation and rotation such as a manipulated object or a part of a human body. In contrast, for pure translations, which can be characterized by space curves traced by a reference point attached to the rigid body, a well-known coordinate-free description that could serve these purposes does exist. The question addressed in this paper is how do these well-known results for space curves generalize to a rigid body motion that involves both translation and rotation?

In particular, a space curve represented by its parametrized coordinates $\mathbf{r}(x(t), y(t), z(t))$ with $0 \leq t \leq t_f$ is completely characterized by three invariant scalars: arc length $s(t)$, curvature $\kappa(t)$, and torsion $\tau(t)$. In many applications parameter t corresponds to time. In this case $s(t)$, $\kappa(t)$, and $\tau(t)$ constitute a unique differential *time-based* description² of the space curve that contains *both the geometric and temporal* information necessary to produce a motion trajectory as a function of time that corresponds to $\mathbf{r}(t)$, up to a Euclidean transformation defined by a given starting point $\mathbf{r}(0)$ and initial orientation of the Frenet frame [7]. In some applications only the *geometric* information is relevant and then the coordinate-free description is stripped from its *temporal* information by inverting the relation $s(t)$ and substituting parameter t by the arc length. This procedure yields two geometric invariants $\kappa(s)$ and $\tau(s)$. Furthermore, to obtain a description that is independent of the linear scale, arc length could be scaled to 1 by dividing it by total arc length $s(t_f)$, while $\kappa(s)$ and $\tau(s)$ are multiplied by $s(t_f)$. This yields two *dimensionless geometric invariants*, $\bar{\kappa}(\bar{s})$ and $\bar{\tau}(\bar{s})$, where the bar denotes a dimensionless quantity. To produce a motion trajectory in this case, we need to provide a time scale t_f , a linear scale $s(t_f)$, and a time function $\bar{s}(\bar{t})$ with $0 \leq \bar{s}, \bar{t} \leq 1$, in

²The description is unique if *signed* curvature and torsion are defined.

addition to the starting point and initial orientation of the Frenet frame.

This paper generalizes the coordinate-free differential description of space curves to full 3D rigid body motion. The description consists of six time-based invariants. Two of the invariants correspond to rotational velocity about and translational velocity along the *instantaneous screw axis* (ISA); the other four invariants correspond to rotational and translational velocities, which model the spatial motion of the ISA. The six invariants suffice to produce a rigid body motion trajectory as a function of time that is unique up to two Euclidean transformations defined by the initial pose of the rigid body and the initial pose of a frame attached to the ISA. The six time-based invariants can be stripped from the temporal information yielding five independent geometric invariants. Given a coordinate description of a rigid body motion, the paper presents (i) analytic formulas to compute the invariants at each time instant, and (ii) a numerical algorithm to reconstruct the motion trajectory from its invariant description.

1.1 Previous Work. Motion trajectory based motion description has extensively been studied in recent research. Wu and Li [8] provided a recent overview. However, almost all references, including Ref. [8] itself, focus on the description of curves, not full 3D rigid body motion involving simultaneous translation and rotation, for which previous work by kinematicians provides a solid background.

From the work of Chasles [9], it is known that any motion is characterized instantaneously to the first-order by the instantaneous screw axis. In fact, Ceccarelli [10] showed that Mozzi [11] defined the screw axis already in 1763. Skreiner [12] studied the higher order properties of motion based on the local properties of the *axodes*, the ruled surfaces generated by the ISA, one in the fixed member and one in the moving member, and of the *line of striction*, the space curve traced by the *central point*. Veldkamp [13] studied the acceleration distribution in spatial motion using the angular acceleration axes. In the discussion of this paper Skreiner [14] modeled the rate of change of the ISA by means of a screw motion and considered several special cases. Bokelberg et al. [15] introduced the concept of *differential screw* to model the difference between two successive instantaneous screws. Hence Skreiner [14] and Bokelberg et al. [15] modeled the spatial motion of the ISA up to the first-order.

A method for locating instantaneous screw axes and determining their properties has been developed by Phillips and Hunt [16]. Other authors have developed efficient algorithms to compute rigid body velocity and/or acceleration descriptors based on position, velocity, and acceleration data for individual points of the moving body [17–21]. Fenton and Willgoss [22] compared five methods for determining the screw parameters of infinitesimal rigid body motion from position and velocity data of individual points.

Veldkamp [23] and Bottema and Roth [24] defined invariant numbers that locally characterize the trajectory of any point attached to a moving rigid body up to an arbitrary order. Modeling the time-based (kinematic) properties of these point trajectories up to first order requires two time-based invariants, the second order requires four additional invariants, and third and higher orders each require six additional invariants. Modeling only the intrinsic geometric properties of the point trajectories requires one, three, and five geometric invariants for first, second and third and higher orders, respectively. The time-based invariants are derived from the trajectories of individual points attached to the rigid body. Furthermore, Roth [25] showed how to find the geometric invariants from the time-based invariants. There are two major differences with the approach presented in this paper. First, Bottema and Roth [24] concentrated on *instantaneous* time-based and geometric invariants that characterize the *local* description of point trajectories, whereas this paper focuses on an invariant description of a *complete trajectory* executed by a rigid body. In particular, it is shown how to generate or reproduce a complete rigid body

motion trajectory from a set of invariant functions of time or another parameter. Second, the sets of invariant numbers proposed by Bottema and Roth do not provide a *complete and minimal* description of the motion trajectory. This is understood as follows. Consider the local description up to second order. The time-based description consists of six invariant numbers. Suppose these numbers are known along the trajectory, for example, as a function of time. One of the second-order invariants (ϵ_2) is the derivative of a first-order invariant (ω); hence, it does not contain independent information. And hence, with six numbers, this second-order description can never be complete, while any higher-order description will be nonminimal. On the other hand, the geometric description up to second order is based on four invariant numbers. Since at least five invariants are needed, the second-order description is not complete, while higher-order descriptions are again nonminimal.

Other authors [26–30] have further investigated the relationship between instantaneous invariants and the local properties of point and line trajectories for planar, spherical, or spatial motion. The main interest of these papers was to study the properties of mechanisms in view of mechanism design and not to find a minimal and complete invariant description of a rigid body motion trajectory, as is the focus in this paper.

The approach in this paper is based on a model for the spatial motion of the ISA and is inspired by the Denavit–Hartenberg convention [31] to model the geometric relation between successive joints in a mechanism.

1.2 Paper Overview. This paper is structured as follows. Section 2 defines time-based invariants, provides analytic formulas to derive them from the motion data, and shows how to reconstruct the motion trajectory from the time-based invariants. Section 3 analyzes the properties of the time-based invariants and derives geometric invariants from the time-based invariants. Section 4 presents a numerical example. Finally, Sec. 5 states the conclusions and discusses future work.

2 Time-Based Invariants

2.1 Definition. Any motion is characterized instantaneously to the first order by the instantaneous screw axis [9,11]. The rotational velocity about and translational velocity along the ISA are denoted by two scalars, ω_1 and v_1 , respectively. The first two invariants of the rigid body motion correspond to ω_1 and v_1 , which are, in general, functions of time

$$i_1 \triangleq \omega_1(t), \quad i_2 \triangleq v_1(t) \quad (3)$$

Four other invariants model the spatial motion of the ISA. Figure 1 shows the ISA at three consecutive time instants $t-\Delta t$, t and $t+\Delta t$. Assign a frame to each ISA as follows: the x -axis lies along the ISA, while the y -axis lies along the common normal between the ISA at the current instant and the ISA at the next instant. The orientation of both axes is chosen such that there is no discontinuity in their orientation between subsequent time instants. The origin \mathbf{o} of the ISA frame is known as the *central point* [12,13] or *striction point* [24].

The motion of the ISA between two consecutive time instants $t-\Delta t$ and t consists of a rotation about $y(t-\Delta t)$ over an angle $\Delta\theta_2(t)$ and a translation along $y(t-\Delta t)$ over a distance $\Delta d_2(t)$. The motion of the frame attached to the ISA between two consecutive time instants $t-\Delta t$ and t consists of two additional components: a rotation about $x(t)$ over an angle $\Delta\theta_3(t)$ and a translation along $x(t)$ over a distance $\Delta d_3(t)$.

Hence, the instantaneous motion of the ISA and the frame attached to it is completely described by defining four velocities

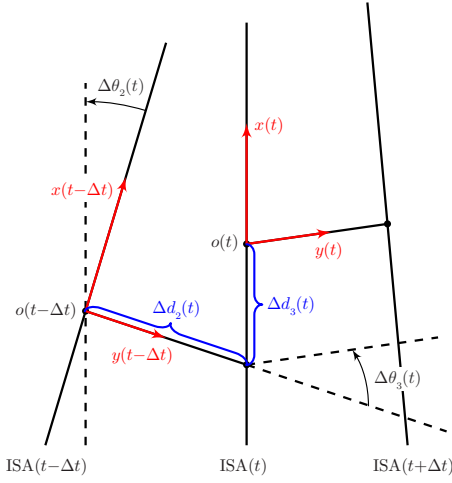


Fig. 1 The instantaneous screw axis at three consecutive time instants

$$\omega_2(t) = \lim_{\Delta t \rightarrow 0} \frac{\Delta \theta_2(t)}{\Delta t} \quad (4)$$

$$v_2(t) = \lim_{\Delta t \rightarrow 0} \frac{\Delta d_2(t)}{\Delta t} \quad (5)$$

$$\omega_3(t) = \lim_{\Delta t \rightarrow 0} \frac{\Delta \theta_3(t)}{\Delta t} \quad (6)$$

$$v_3(t) = \lim_{\Delta t \rightarrow 0} \frac{\Delta d_3(t)}{\Delta t} \quad (7)$$

While ω_2 and v_2 model the first-order kinematics of the ISA, the y-axis is known as the *second-order instantaneous screw axis* [32]. On the other hand, ω_3 and v_3 model (part of) the second-order kinematics of the ISA (together with $\dot{\omega}_2$ and \dot{v}_2). Since the ISA is uniquely defined at every time instant, the four velocities are invariant properties of the motion. They are denoted by i_3 to i_6

$$i_3 \triangleq \omega_2(t), \quad i_4 \triangleq v_2(t), \quad i_5 \triangleq \omega_3(t), \quad i_6 \triangleq v_3(t) \quad (8)$$

2.2 Closed-Form Formulas. This subsection shows how to calculate the invariants $i_l(t)$, with $l=1, \dots, 6$, from the twist of the rigid body, given as ${}_{\text{ref}}\mathbf{t}^{\text{ref}} = (\boldsymbol{\omega}^T \mathbf{v}^T)^T$. If $\{\text{ref}\} = \{w\}$, the reference point for the translational velocity is the point attached to the rigid body that instantaneously coincides with the origin of the world frame. In this case invariants i_l , with $i=3, \dots, 6$, model the motion of the ISA with respect to the world. On the other hand, if $\{\text{ref}\} = \{\text{rb}\}$, the reference point for the translational velocity corresponds to the origin of a body-fixed reference frame. In this case invariants i_l , with $i=3, \dots, 6$, model the motion of the ISA with respect to the rigid body (see also Sec. 3.2).

This subsection assumes the general case where $\|\boldsymbol{\omega} \times \dot{\boldsymbol{\omega}}\| \neq 0$, that is, the case where the rigid body has a nonzero rotational velocity and the ISA has a nonconstant orientation.

Since the rotational velocity of a rigid body is uniquely defined, we have

$$\omega_1 = \pm \|\boldsymbol{\omega}\| \quad (9)$$

where the sign of ω_1 depends on the orientation of the ISA. The unit vector along the ISA is given by

$$\mathbf{e}_x = \pm \frac{\boldsymbol{\omega}}{\|\boldsymbol{\omega}\|} \quad (10)$$

Hence, the signed value for ω_1 follows from

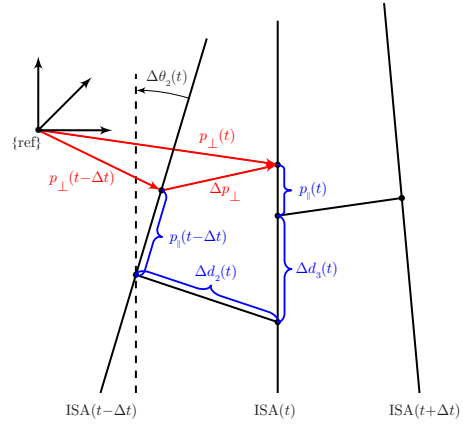


Fig. 2 Decomposition of $\Delta \mathbf{p}_\perp$

$$\omega_1 = \boldsymbol{\omega} \cdot \mathbf{e}_x \quad (11)$$

where, as explained in Sec. 2.1, the sign of \mathbf{e}_x is chosen such that $\mathbf{e}_x(t)$ is a continuous function of time.

Projecting the velocity of any point attached to the rigid body onto the ISA yields v_1

$$v_1 = \mathbf{v} \cdot \mathbf{e}_x \quad (12)$$

$$= \pm \frac{\mathbf{v} \cdot \boldsymbol{\omega}}{\|\boldsymbol{\omega}\|} \quad (13)$$

ω_2 is found from Eq. (4) as

$$\omega_2 = \pm \frac{\|\boldsymbol{\omega} \times \dot{\boldsymbol{\omega}}\|}{\|\boldsymbol{\omega}\|^2} \quad (14)$$

Accordingly, the unit vector normal to the osculating plane of the ISA is expressed as

$$\mathbf{e}_y = \pm \frac{\boldsymbol{\omega} \times \dot{\boldsymbol{\omega}}}{\|\boldsymbol{\omega} \times \dot{\boldsymbol{\omega}}\|} \quad (15)$$

The sign of \mathbf{e}_y is again chosen such that $\mathbf{e}_y(t)$ is a continuous function of time and consequently the signed value for ω_2 follows from:

$$\omega_2 = \frac{(\boldsymbol{\omega} \times \dot{\boldsymbol{\omega}}) \cdot \mathbf{e}_y}{\|\boldsymbol{\omega}\|^2} \quad (16)$$

Derivation of v_2 involves three steps. First, find an expression for \mathbf{p}_\perp , the position vector from the origin of $\{\text{ref}\}$ and perpendicular to the ISA (see Fig. 2)

$$\mathbf{p}_\perp = \frac{\boldsymbol{\omega} \times \mathbf{v}}{\|\boldsymbol{\omega}\|^2} \quad (17)$$

This expression is easily verified as follows:

$$\mathbf{v} = \pm \frac{\boldsymbol{\omega}}{\|\boldsymbol{\omega}\|} v_1 + \mathbf{p}_\perp \times \boldsymbol{\omega} \quad (18)$$

hence

$$\boldsymbol{\omega} \times \mathbf{v} = \pm \frac{\boldsymbol{\omega} \times \boldsymbol{\omega}}{\|\boldsymbol{\omega}\|} v_1 + \boldsymbol{\omega} \times (\mathbf{p}_\perp \times \boldsymbol{\omega}) \quad (19)$$

$$= \|\boldsymbol{\omega}\|^2 \mathbf{p}_\perp \quad (20)$$

Next, calculate the time derivative of \mathbf{p}_\perp

$$\dot{\mathbf{p}}_{\perp} = \frac{(\dot{\boldsymbol{\omega}} \times \mathbf{v} + \boldsymbol{\omega} \times \dot{\mathbf{v}}) \cdot \|\boldsymbol{\omega}\|^2 - 2(\boldsymbol{\omega} \times \mathbf{v}) \cdot (\boldsymbol{\omega} \cdot \dot{\boldsymbol{\omega}})}{\|\boldsymbol{\omega}\|^4} \quad (21)$$

$\dot{\mathbf{p}}_{\perp}$ has a component in the xz -plane due to the rotation of the ISA, as well as a component along the y -axis due to the translation of the ISA, see Fig. 2. The latter is easily verified, since $\mathbf{p}_{\perp}(t) \perp \text{ISA}(t)$ and $\mathbf{p}_{\perp}(t+\Delta t) \perp \text{ISA}(t+\Delta t)$. Hence, if $\text{ISA}(t) \parallel \text{ISA}(t+\Delta t)$ then $\dot{\mathbf{p}}_{\perp}(t) \perp \text{ISA}(t) \parallel \text{ISA}(t+\Delta t)$. Consequently, in a third step, v_2 is found by projecting $\dot{\mathbf{p}}_{\perp}$ onto the y -axis

$$v_2 = \mathbf{e}_y \cdot \dot{\mathbf{p}}_{\perp} \quad (22)$$

Substituting Eqs. (15) and (21) into Eq. (22) yields a closed-form expression for v_2

$$v_2 = \pm \frac{(\boldsymbol{\omega} \times \dot{\boldsymbol{\omega}})}{\|\boldsymbol{\omega} \times \dot{\boldsymbol{\omega}}\|} \cdot \left[\frac{(\dot{\boldsymbol{\omega}} \times \mathbf{v} + \boldsymbol{\omega} \times \dot{\mathbf{v}}) \cdot \|\boldsymbol{\omega}\|^2 - 2(\boldsymbol{\omega} \times \mathbf{v}) \cdot (\boldsymbol{\omega} \cdot \dot{\boldsymbol{\omega}})}{\|\boldsymbol{\omega}\|^4} \right] \quad (23)$$

ω_3 corresponds to the rotation of the y -axis and is, hence, found in a similar way as ω_2 , that is, by replacing $\boldsymbol{\omega}$ in Eq. (14) by $\boldsymbol{\omega} \times \dot{\boldsymbol{\omega}}$ ³

$$\omega_3 = \pm \frac{\|(\boldsymbol{\omega} \times \dot{\boldsymbol{\omega}}) \times (\boldsymbol{\omega} \times \dot{\boldsymbol{\omega}})\|}{\|\boldsymbol{\omega} \times \dot{\boldsymbol{\omega}}\|^2} \quad (24)$$

$$= \pm \frac{\|\boldsymbol{\omega}\|}{\|\boldsymbol{\omega} \times \dot{\boldsymbol{\omega}}\|^2} \cdot |(\boldsymbol{\omega} \times \dot{\boldsymbol{\omega}}) \cdot \dot{\boldsymbol{\omega}}| \quad (25)$$

The signed value of ω_3 follows by replacing $\boldsymbol{\omega}$ in Eq. (16) by $\boldsymbol{\omega} \times \dot{\boldsymbol{\omega}}$ and \mathbf{e}_y by \mathbf{e}_x

$$\omega_3 = \frac{(\boldsymbol{\omega} \times \dot{\boldsymbol{\omega}}) \times (\boldsymbol{\omega} \times \dot{\boldsymbol{\omega}})}{\|\boldsymbol{\omega} \times \dot{\boldsymbol{\omega}}\|^2} \cdot \mathbf{e}_x \quad (26)$$

Finally, the derivation of v_3 involves two steps. First, note that the component of $\dot{\mathbf{p}}_{\perp}$ in the xz -plane is due to the rotation of the ISA. The origin of the ISA frame is found by projecting $\dot{\mathbf{p}}_{\perp}$ onto the z -axis and dividing by ω_2 , see Fig. 2. This yields the x -coordinate p_{\parallel} along the ISA of the intersection point with \mathbf{p}_{\perp}

$$p_{\parallel} = -\frac{\mathbf{e}_z \cdot \dot{\mathbf{p}}_{\perp}}{\omega_2} \quad (27)$$

where $\mathbf{e}_z = \mathbf{e}_x \times \mathbf{e}_y$ yielding

$$\mathbf{e}_z = \pm \frac{\boldsymbol{\omega} \times (\boldsymbol{\omega} \times \dot{\boldsymbol{\omega}})}{\|\boldsymbol{\omega}\| \cdot \|\boldsymbol{\omega} \times \dot{\boldsymbol{\omega}}\|} \quad (28)$$

v_3 is found as the difference between the component of $\dot{\mathbf{p}}_{\perp}$ along the ISA and the time derivative of p_{\parallel}

$$v_3 = \mathbf{e}_x \cdot \dot{\mathbf{p}}_{\perp} - \dot{p}_{\parallel} \quad (29)$$

A closed-form expression for v_3 , shown in Appendix A, is found by substituting Eqs. (28), (21), and (14) into Eq. (27), taking the time derivative and substituting the result into Eq. (29) together with Eqs. (10) and (21).

2.3 Special Cases

2.3.1 Pure Translation. In this case $\boldsymbol{\omega} = \mathbf{0}$, the location of the ISA is not defined, and the orientation of the ISA is determined by the translational velocity \mathbf{v} , which is the same for every point attached to the rigid body. Hence, $\omega_1 = 0$ and $v_1 = \pm \|\mathbf{v}\|$, while in Eqs. (14) and (25) $\boldsymbol{\omega}$ is replaced by \mathbf{v}

$$\omega_2 = \pm \frac{\|\mathbf{v} \times \dot{\mathbf{v}}\|}{\|\mathbf{v}\|^2} \quad (30)$$

$$\omega_3 = \pm \frac{\mathbf{v}}{\|\mathbf{v} \times \dot{\mathbf{v}}\|^2} \cdot |(\mathbf{v} \times \dot{\mathbf{v}}) \cdot \ddot{\mathbf{v}}| \quad (31)$$

Note that Eqs. (30) and (31) are related to the formulas for the curvature κ and torsion τ of a space curve, respectively

$$\omega_2 = \pm \kappa \|\mathbf{v}\|, \quad \omega_3 = \pm \tau \|\mathbf{v}\| \quad (32)$$

Finally, v_2 and v_3 are not defined in the case of pure translation because the location of the ISA is not defined.

2.3.2 ISA With Constant Orientation. In this case $\|\boldsymbol{\omega} \times \dot{\boldsymbol{\omega}}\| = 0$. Hence, $\omega_2 = 0$ and $\dot{\mathbf{p}}_{\perp}$ has only a component along the y -axis. Consequently

$$v_2 = \pm \|\dot{\mathbf{p}}_{\perp}\| \quad (33)$$

$$\omega_3 = \frac{\|\dot{\mathbf{p}}_{\perp} \times \ddot{\mathbf{p}}_{\perp}\|}{\|\dot{\mathbf{p}}_{\perp}\|^2} \quad (34)$$

ω_3 is not defined in case the ISA is fixed in space, since then $\|\dot{\mathbf{p}}_{\perp}\| = 0$. Finally, v_3 is not defined, since the origin of the ISA frame is not uniquely defined in the case of an ISA with constant orientation.

2.4 Trajectory Reconstruction. The reconstruction of the motion trajectory from a set of time-based invariants $i_l(t)$ with $l = 1, \dots, 6$ proceeds in three steps.

First, if the ISA is known at time instant $t=0$ and $\omega_2(t)$, $v_2(t)$, $\omega_3(t)$, and $v_3(t)$ are known for $0 \leq t = kT \leq t_f = N_f T$, the pose of the reference frame attached to the ISA at discrete-time instant $k+1$ is calculated from time instant k as [33]

$$\mathbf{I}_{\text{ref}}^{\text{ISA}} T(k+1) = \mathbf{I}_{\text{ref}}^{\text{ISA}} T(k) \Delta T(\Delta \mathbf{p}, \mathbf{e}_{\text{eq}}, \Delta \theta) \quad (35)$$

with

$$\Delta T(\Delta \mathbf{p}, \mathbf{e}_{\text{eq}}, \Delta \theta) = \text{trans}(\Delta \mathbf{p}) \text{rot}(\mathbf{e}_{\text{eq}}, \Delta \theta) \quad (36)$$

and

$$\Delta \mathbf{p} = \mathbf{I}_{\text{ISA}}^{\text{ISA}} \mathbf{v}(k) T \quad (37)$$

$$\mathbf{e}_{\text{eq}} = \frac{\mathbf{I}_{\text{ISA}}^{\text{ISA}} \boldsymbol{\omega}(k)}{\|\mathbf{I}_{\text{ISA}}^{\text{ISA}} \boldsymbol{\omega}(k)\|} \quad (38)$$

$$\Delta \theta = \|\mathbf{I}_{\text{ISA}}^{\text{ISA}} \boldsymbol{\omega}(k)\| T \quad (39)$$

Here $\mathbf{I}_{\text{ISA}}^{\text{ISA}} \boldsymbol{\omega}^T \mathbf{I}_{\text{ISA}}^{\text{ISA}} \mathbf{v}^T)^T = (\omega_3 \ \omega_2 \ 0 \ v_3 \ v_2 \ 0)^T$ denotes the twist of frame {ISA} expressed in {ISA}, T is the integration step, and $\text{rot}(\mathbf{e}_{\text{eq}}, \Delta \theta)$ and $\text{trans}(\Delta \mathbf{p})$ denote a rotation about an axis with direction \mathbf{e}_{eq} over an angle $\Delta \theta$ and a translation over a vector $\Delta \mathbf{p}$, respectively. Reference frame {ref} is either the world frame {w} or a frame {rb} rigidly attached to the rigid body, depending on whether the motion of the ISA is defined with respect to the world or with respect to the moving body.

Next, with the ISA known at each time instant k , the twist of the rigid body with respect to the world is calculated as

$$\mathbf{I}_{\text{ref}}^{\text{rb}} \mathbf{t}_w^{\text{ref}}(k) = \mathbf{I}_{\text{ref}}^{\text{ISA}} \mathbf{S}(k) \mathbf{I}_{\text{ISA}}^{\text{ISA}} \mathbf{t}_w^{\text{ISA}}(k) \quad (40)$$

where $\mathbf{I}_{\text{ISA}}^{\text{rb}} \mathbf{t}_w^{\text{ISA}} = (\omega_1 \ 0 \ 0 \ v_1 \ 0 \ 0)^T$, and screw transformation matrix $\mathbf{I}_{\text{ref}}^{\text{ISA}} \mathbf{S}$ is known from $\mathbf{I}_{\text{ref}}^{\text{ISA}} T$.

Finally, if the pose of the rigid body is known at $t=0$, the pose of the rigid body with respect to the world for $0 \leq t = kT \leq t_f = N_f T$ is calculated from $\mathbf{I}_{\text{ref}}^{\text{rb}} \mathbf{t}_w^{\text{ref}} = \mathbf{I}_{\text{ref}}^{\text{rb}} \boldsymbol{\omega}^T \mathbf{I}_{\text{ref}}^{\text{rb}} \mathbf{v}^T)^T$ similarly, as in Eq. (35), if {ref}={rb} or with the multipliers in reverse order if {ref}={w} [33].

3 Properties and Derived Invariants

3.1 Uniqueness, Completeness, and Minimal Set. Formulas (9), (13), (14), (23), (25), and (A1) yield six scalar functions, which are uniquely defined except for their sign. This causes am-

³Making use of $\boldsymbol{\omega} \times \dot{\boldsymbol{\omega}} = 0$, $\mathbf{a} \times (\mathbf{b} \times \mathbf{c}) = \mathbf{b}(\mathbf{a} \cdot \mathbf{c}) - \mathbf{c}(\mathbf{a} \cdot \mathbf{b})$ and $(\boldsymbol{\omega} \times \dot{\boldsymbol{\omega}}) \cdot \boldsymbol{\omega} = 0$.

biguity if the scalars have to be computed at *only one* time instant.⁴ If, however, the scalars have to be computed for a rigid body motion over a *time period*, uniqueness is obtained by imposing continuity of the orientation of the ISA and its normal, represented by e_x and e_y , by switching to formulas (11), (12), (16), (22), (26), and (29) and by imposing a convention for the sign of ω_1 and ω_2 at $t=0$, which fixes the initial orientation of e_x and e_y . With these measures every rigid body motion has a unique signature consisting of the six invariants $i_l(t)$. On the other hand, every set of invariants corresponds to a rigid body motion that is unique up to two Euclidean transformations defined by the initial pose of the rigid body and the initial pose of the ISA, as shown by the procedure in Sec. 2.4.

As a corollary, together with the initial poses of the ISA and of the moving body, the six invariants constitute a *complete* description of the rigid body motion.

Since the invariant description is able to describe any six degree of freedom (6dof) rigid body motion with only six functions, it is obviously a *minimal set* of invariants.

3.2 Invariance With Respect to the Twist Reference Frame. The input to the closed-form formulas is the twist defined with respect to some reference frame {ref}. As explained in Sec. 2.2, the interpretation of the invariants depends on whether {ref} is a fixed frame attached to the world or a body-fixed frame attached to the moving body. The relation between both sets of invariants is

$$i_l^{\text{rb}} = i_l^{\text{w}} \quad \text{for } l = 1, \dots, 4 \quad (41)$$

$$\omega_3^{\text{rb}} = \omega_3^{\text{w}} - \omega_1, \quad v_3^{\text{rb}} = v_3^{\text{w}} - v_1 \quad (42)$$

This relation, in which the superscripts refer to whether {ref} = {rb} or {ref} = {w} is obvious, since the relative motions of the moving body, the ISA, and the world with respect to each other are governed by

$${}^{\text{ISA}}\mathbf{t}_{\text{rb}} = {}^{\text{ISA}}\mathbf{t}_{\text{w}} - {}^{\text{rb}}\mathbf{t}_{\text{w}} \quad (43)$$

and since the motion of the rigid body with respect to the world, ${}^{\text{rb}}\mathbf{t}_{\text{w}}$, corresponds to ω_1 and v_1 about and along the ISA.

Apart from the difference between a moving or a fixed reference frame, the calculation of i_l with $l=1, \dots, 6$ is invariant for the choice of the reference frame. This is intuitively evident from Chasles' theorem, but it can also be proven mathematically. *Rotation* of the reference frame does not affect i_l because rotation does not affect the norm of a vector, nor the angle between vectors; hence, the norm of a vector cross product, as well as the value of the dot product, is preserved under a rotation. On the other hand, while a *translation* does not affect the coordinates of ω , it does affect the coordinates of \mathbf{v} : $\mathbf{v}^* = \mathbf{v} + \mathbf{u} \times \omega$, where \mathbf{u} represents the translation of the reference frame. Hence, as follows from Eqs. (9), (14), and (25), ω_1 , ω_2 , and ω_3 remain unchanged under a translation of the world reference frame. On the other hand, the expressions for v_1 , v_2 , and v_3 use \mathbf{v} and should be verified for invariance. Given Eq. (10), invariance of v_1 follows from

$$(\mathbf{v} + \mathbf{u} \times \omega) \cdot \mathbf{e}_x = \mathbf{v} \cdot \mathbf{e}_x \quad (44)$$

Appendix B contains verification of the invariance of v_2 and v_3 .

3.3 Inverse and Reverse Motion. Inverse motion refers to relative motion of the world with respect to moving body instead of the other way around. While this causes the input twist to the closed-form formulas to change sign, the ISA still executes the same motion. Hence, only ω_1 and v_1 change sign. By inverting the orientation of the ISA, this sign change is compensated, but then ω_3 and v_3 change signs. Hence

$$i_l^{\text{inv}} = i_l \quad \text{for } l = 1, \dots, 4 \quad (45)$$

$$\omega_3^{\text{inv}} = -\omega_3, \quad v_3^{\text{inv}} = -v_3 \quad (46)$$

Reverse motion refers to executing the motion in reverse direction. This causes both the twist of the moving body and of the ISA to change sign, such that all invariants change sign. By inverting the orientation of the ISA and of the common normal however all sign changes are compensated. Hence

$$i_l^{\text{rev}}(t) = i_l(t_f - t) \quad \text{for } l = 1, \dots, 6 \quad (47)$$

3.4 Invariance With Respect to Time, Linear, and/or Angular Scale. To compare motions executed with different velocities it is interesting to make the invariants independent of the time scale, that is, to make them independent of the *average* velocity with which the motion is executed but keep the dependence on the motion *profile*. To this end consider the dimensionless time

$$\bar{t} = \frac{t}{t_f} \quad (48)$$

where t_f is the duration of the rigid body motion and is referred to as the *time scale*. Multiplying $i_l(t)$ by t_f and substituting t by \bar{t} results in invariants that are independent of the time scale.

Similarly, to compare motions with different amplitudes, it is interesting to make the invariants independent of linear and/or angular scale. While invariance with respect to linear scale could be practically relevant in many applications, invariance with respect to angular scale is probably only relevant in a few special cases, such as a pure orientation around a fixed point or a pure screw motion, see Sec. 3.7. To this end define the angular and linear scale of the motion as

$$\Theta = \int_0^{t_f} |\omega_1| dt \quad (49)$$

$$L = \int_0^{t_f} |v_1| dt \quad (50)$$

and divide $\omega_i(\bar{t})$ and/or $v_i(\bar{t})$ by Θ and L , respectively. Making the invariants independent of time, linear, and angular scale results in *dimensionless time-based invariants*, which are denoted by $\bar{i}_l(\bar{t})$, $\bar{\omega}_i(\bar{t})$, or $\bar{v}_i(\bar{t})$ further on

$$\bar{\omega}_i(\bar{t}) = \frac{\omega_i(t = \bar{t} \cdot t_f)}{\Theta}, \quad \bar{v}_i(\bar{t}) = \frac{v_i(t = \bar{t} \cdot t_f)}{L} \quad (51)$$

3.5 Invariance With Respect to Motion Profile. To eliminate the influence of the motion profile with which the motion is executed, the invariants have to be expressed in terms of a geometric *degree of advancement* of the rigid body motion, $\xi(t)$, instead of time. For a space curve a natural choice for ξ is arc length s . For a rigid body motion no natural choice exists. Often $\dot{\xi}(t)$ is chosen as $|\omega_1(t)|$ [25]. A basic requirement for a degree of advancement is however that $\dot{\xi}(t)$ is nonzero as long as the rigid body moves. Hence, the degree of advancement should also be nonzero at instances where the rigid body undergoes a pure translation or a pure rotation. Therefore, the degree of advancement should be a combination of the advancement of the rigid body translation and the rigid body rotation. Here, a linear combination is proposed

$$\dot{\xi}(t) = w \frac{|\omega_1(t)|}{\Theta_s} + (1 - w) \frac{|v_1(t)|}{L_s} \quad (52)$$

where Θ_s and L_s represent user-defined scaling factors with dimensions of angle and length, respectively, and $0 \leq w \leq 1$ is a user-defined dimensionless weight. Hence the degree of advance-

⁴The same occurs in curvature theory, where only positive generalized curvatures are defined. For example for a 3D space curve, only positive values of curvature are defined and the normal direction of the Frenet frame flips over 180 deg accordingly.

ment $\xi(t)$ is dimensionless. Once the scales and the weight have been fixed, dividing $i_f(t)$ by the rate of advancement (52), inverting $\xi(t)$, and substituting t by ξ , results in six *geometric invariants*, which contain the geometry of the rigid body motion without the effect of time. Further on the geometric invariants are written with capital letters $I_i(\xi)$, $\Omega_i(\xi)$, or $V_i(\xi)$

$$\Omega_i(\xi) = \frac{\omega_i(t(\xi))}{\dot{\xi}(t(\xi))}, \quad V_i(\xi) = \frac{v_i(t(\xi))}{\dot{\xi}(t(\xi))} \quad (53)$$

Only five geometric invariants are independent, since $\Omega_1(\xi)$ and $V_1(\xi)$ are constrained by Eq. (52), which after division by $\dot{\xi}(t)$ becomes

$$1 = w \frac{|\Omega_1(\xi)|}{\Theta_s} + (1-w) \frac{|V_1(\xi)|}{L_s} \quad (54)$$

Therefore it is common to replace $\Omega_1(\xi)$ and $V_1(\xi)$ by a single invariant $p_1(\xi)$, which is known as the pitch of the instantaneous screw motion

$$p_1(\xi) = \frac{V_1(\xi)}{\Omega_1(\xi)} = \frac{v_1(t(\xi))}{\omega_1(t(\xi))} \quad (55)$$

The sixth invariant is $\xi(t)$, which contains the temporal information.

To compare motions with different angular or linear amplitudes, the degree of advancement can be scaled to 1 by selecting $\Theta_s = \Theta$ and $L_s = L$, as defined in Eqs. (49) and (50), yielding the normalized degree of advancement $\bar{\xi}(t)$. This procedure however breaks down if the entire motion consists of a pure translation or a pure rotation, because $\Theta = 0$ or $L = 0$, respectively. In such case w is set equal to 1 or 0 in Eq. (52), respectively. Furthermore, dividing $\omega_i(t)$ and $v_i(t)$ by $\dot{\xi}$ and dividing them by Θ and/or L , respectively, inverting $\bar{\xi}(t)$, and substituting t by $\bar{\xi}$ results in six *dimensionless geometric invariants*. Further on the dimensionless geometric invariants are written as $\bar{I}_i(\bar{\xi})$, $\bar{\Omega}_i(\bar{\xi})$, or $\bar{V}_i(\bar{\xi})$

$$\bar{\Omega}_i(\bar{\xi}) = \frac{\omega_i(t(\bar{\xi}))}{\dot{\bar{\xi}}(t(\bar{\xi}))\Theta}, \quad \bar{V}_i(\bar{\xi}) = \frac{v_i(t(\bar{\xi}))}{\dot{\bar{\xi}}(t(\bar{\xi}))L} \quad (56)$$

Using the definitions of $\bar{\Omega}_i(\bar{\xi})$ and $\bar{V}_i(\bar{\xi})$, constraint (54) reduces to

$$1 = w|\bar{\Omega}_1(\bar{\xi})| + (1-w)|\bar{V}_1(\bar{\xi})| \quad (57)$$

while the temporal invariant is conveniently written as a function of dimensionless time: $\bar{\xi}(\bar{t})$.

To reconstruct a motion trajectory starting from the dimensionless geometric constraints, given a time scale t_f , a linear and an-

Table 1 Invariants for a left-handed screwing motion

Running parameter	ω_1	v_1	
A	$0 \leq t \leq t_f$	$\omega_1(t) = \frac{\alpha}{t_f} \bar{\xi}'\left(\frac{t}{t_f}\right)$	$v_1(t) = \frac{p\alpha}{t_f} \bar{\xi}'\left(\frac{t}{t_f}\right)$
B	$0 \leq \bar{t} \leq 1$	$\omega_1(\bar{t}) = \alpha \bar{\xi}'(\bar{t})$	$\bar{v}_1(\bar{t}) = -\bar{\xi}'(\bar{t})$
C	$0 \leq \xi \leq \xi_f$	$\Omega_1(\xi) = \frac{2}{1+ p }$	$V_1(\xi) = \frac{2p}{1+ p }$
D	$0 \leq \bar{\xi} \leq 1$	$\Omega_1(\bar{\xi}) = \alpha$	$\bar{V}_1(\bar{\xi}) = -1$
E	$0 \leq \bar{\xi} \leq 1$	$\bar{\Omega}_1(\bar{\xi}) = 1$	$\bar{V}_1(\bar{\xi}) = -1$

gular scale L and Θ , and a motion profile $\bar{\xi}(\bar{t})$, the time-based invariants are first reconstructed by inverting Eq. (56)

$$\omega_i(t) = \bar{\Omega}_i\left(\bar{\xi}\left(\bar{t} = \frac{t}{t_f}\right)\right) \bar{\xi}'\left(\bar{t} = \frac{t}{t_f}\right) \frac{\Theta}{t_f} \quad (58)$$

$$v_i(t) = \bar{V}_i\left(\bar{\xi}\left(\bar{t} = \frac{t}{t_f}\right)\right) \bar{\xi}'\left(\bar{t} = \frac{t}{t_f}\right) \frac{L}{t_f}, \quad (59)$$

where $\bar{\xi}'$ represents the derivative with respect to \bar{t} , with $\bar{\xi}' = \dot{\bar{\xi}} t_f$. The motion trajectory then follows from the procedure described in Sec. 2.4.

3.6 Example. Sections 3.4 and 3.5 are illustrated with the example of a screwing motion. A left-handed screw is rotated over an angle α in time t_f by applying a dimensionless motion profile $\bar{\xi}(\bar{t})$. The pitch of the screw is $p < 0$. Table 1 summarizes some of the invariant representations defined above. Only ω_1 and v_1 are represented, since, as explained in Sec. 2.3, for a screwing motion ω_2 and v_2 are identically zero, while ω_3 and v_3 are not defined. Following invariants are considered: (A) real amplitudes as a function of time; (B) independent of time scale and linear scale (dimensionless time-based invariants); (C) independent of motion profile (geometric invariants, with $w=0.5$, $\Theta_s=L_s=1$, and hence $\xi_f=0.5(1+|p|)\alpha$); (D) independent of motion profile and linear scale (dimensionless geometric constraints with $w=0.5$, $\Theta_s=\Theta=\alpha$ and $L_s=L=p\alpha$); (E) same as (D), but also made independent of angular scale.

3.7 Signature of Special Motions. Table 2 displays the *signature* of some special rigid body motions, consisting of the dimensionless geometric invariants (made independent of linear and angular scale).

3.8 Invariance With Respect to Occlusion. Occlusion refers to part(s) of the motion that are missing or invisible [8]. Since the time-based invariants $i_f(t)$ are entirely based on local properties, the parts of the motion that are visible can still be used for com-

Table 2 Signature of special motions (“-”: undefined; “=”: constant; and “*”: $|\bar{\Omega}_1|+|\bar{V}_1|=2$)

	w	$\bar{\Omega}_1$	\bar{V}_1	$\bar{\Omega}_2$	\bar{V}_2	$\bar{\Omega}_3$	\bar{V}_3
General motion	0.5	$\bar{\Omega}_1^*$	\bar{V}_1^*	$\bar{\Omega}_2$	\bar{V}_2	$\bar{\Omega}_3$	\bar{V}_3
Planar motion	1	1	0	0	\bar{V}_2	$\bar{\Omega}_3$	-
3D translation	0	0	1	$\bar{\Omega}_2$	-	$\bar{\Omega}_3$	-
Planar translation	0	0	1	$\bar{\Omega}_2$	-	0	-
Linear translation	0	0	1	0	-	-	-
Helical translation	0	0	1	=	-	=	-
Circular translation	0	0	1	=	-	0	-
Cylindrical motion	0.5	$\bar{\Omega}_1^*$	\bar{V}_1^*	0	0	-	-
Screw motion	0.5	1	± 1	0	0	-	-
Rotation fixed axis	1	1	0	0	0	-	-
3D rotation fixed point	1	1	0	$\bar{\Omega}_2$	0	$\bar{\Omega}_3$	0

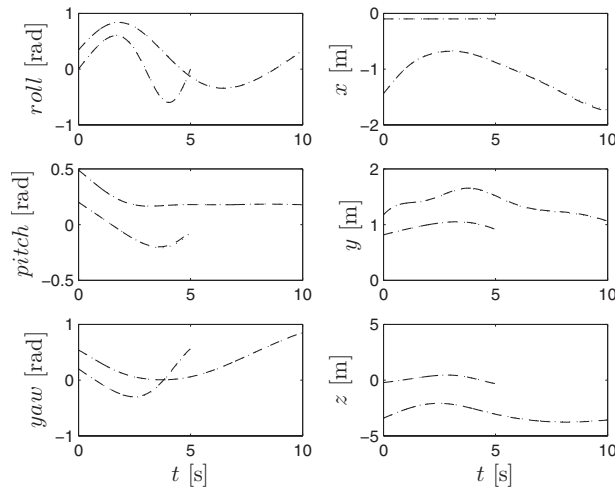


Fig. 3 Pose Coordinates of Motions I and II: given coordinates for motions I and II (dashed); open-loop reconstructed coordinates for motions I and II (dotted); the dashed and dotted lines coincide

parison with models or comparison with other motion trials. For geometric invariants the situation is different because the degree of advancement $\xi(t)$ cannot be calculated by integrating Eq. (52) if parts of the motion are missing. Hence, while it is not possible to derive and compare relations $I_l(\xi)$, it is possible to analyze the cross relations between any two or more I_l and compare these relations with a model or with other motion trials [8].

4 Numerical Example

4.1 Description. Two motions are compared. The motions are assumed to be given by their pose coordinates (dashed lines in Fig. 3). Motion II is geometrically similar to Motion I: the linear amplitude of Motion II is 50% larger than Motion I. But on the other hand, it is two times slower (10 s instead of 5 s); it has another motion profile $\bar{\xi}(\bar{t})$ (Fig. 4); the coordinates are expressed in a different world reference frame; another reference point on the rigid body is chosen to express the x , y , and z coordinates. The

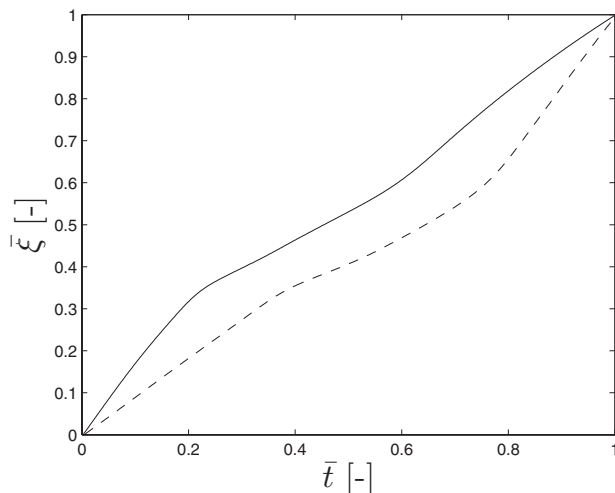


Fig. 4 Dimensionless Degree of Advancement for Motions I (dashed) and II (solid)

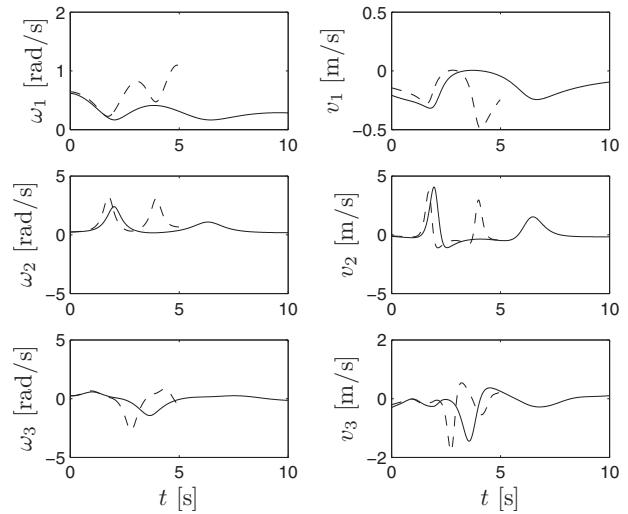


Fig. 5 Time-based Invariants for Motions I (dashed) and II (solid)

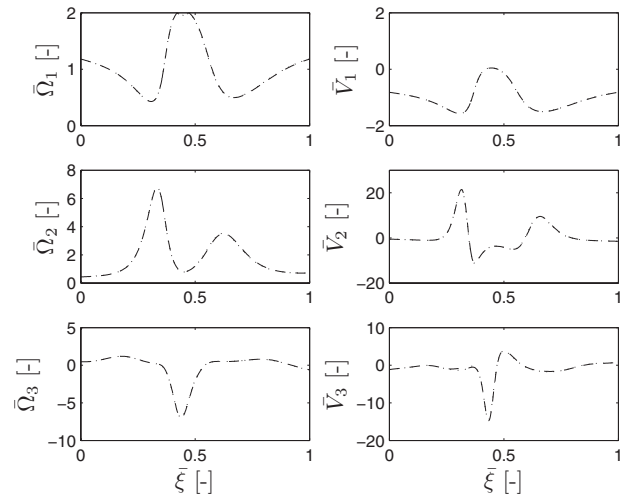


Fig. 6 Dimensionless Geometric Invariants for Motions I (dashed) and II (dotted)

pose coordinates are noiseless. They are converted to twist data expressed in the body-fixed reference frame using numerical differentiation.⁵

4.2 Results. Figure 5 shows the time-based invariants for both Motions I and II as obtained by the analytic solution. On the other hand, Fig. 6 shows the dimensionless geometric invariants for both Motions I and II. Clearly, the invariants for both motions match very well with each other, indicating that apart from linear or angular amplitude both motions are geometrically identical. Hence the invariance properties of the geometric invariants are confirmed.

4.3 Validation. To validate the results, the pose coordinates of the rigid body are reconstructed from the time-based invariants for both Motions I and II. This validation proceeds in three steps, as explained in Sec. 2.4. The results are shown by the dotted lines in Fig. 3. This figure reveals that the reconstructions of the pose

⁵In a practical experiment the twist data are generated from velocity and position measurement data of at least three noncollinear points on the rigid body, for example, using one of the methods compared in Ref. [22]. Obviously, for noiseless data these methods yield the same results as the procedure used in the numerical example.

trajectories are very accurate, keeping in mind that these reconstructions result from a double open-loop integration. Hence the correctness of the analytic formulas to obtain the time-based invariants is verified.

5 Conclusion

This paper presents a minimal invariant coordinate-free description of rigid body motion. Based on a motion model for the instantaneous screw axis, a time-based coordinate-free description consisting of six scalar functions of time is defined. While the time-based functions are independent of the reference frame and of the reference point on the rigid body, they can be made independent of time scale and linear and angular scale by presenting them in dimensionless form. Analytical formulas are derived to obtain these functions from pose or twist coordinates. The information contained in the time-based functions can be split up in temporal information, represented by the motion profile, and geometric information, represented by five independent geometric functions. The geometric functions are shown to be invariant with respect to time scale, motion profile, reference frame, and reference point on the rigid body used to express the translational components of the motion, and when expressed in dimensionless form, they are also invariant with respect to linear and angular scale. A discrete-time algorithm is presented to reconstruct a coordinate representation for a motion trajectory from the time-based or geometric invariants. A numerical example illustrates the

validity of the approach: the analytic formulas yield correct results, and the claimed invariant properties are confirmed.

The analytic formulas have following drawbacks in view of practical use: (i) care has to be taken to impose continuity of the orientation of the ISA and the common normal; (ii) the formulas are sensitive to measurement noise, since they need the second time derivative of the twist components (which, in turn, are usually derived from pose measurements); (iii) several limit cases have to be considered explicitly, which is prone to error in the presence of numerical errors and measurement noise, and (iv) the formulas do not provide a confidence measure for the calculated invariants. Future work consists of overcoming these drawbacks by designing a stochastic recursive filter based on an ISA motion model.

Acknowledgment

The author would like to thank Herman Bruyninckx for pointing to the kinematic literature which helped to position this work against contributions from the past. The reviewers of this paper pointed to a few additional references. Jochem De Schutter and Roel Matthyssen worked out the closed-form expression for v_3 , and Wilm Decré made Figs. 1 and 2. The author gratefully acknowledges the financial support by K.U.Leuven's Concerted Research Action Grant No. GOA/05/10 and K.U.Leuven's CoE Grant No. EF/05/006 Optimization in Engineering Center (OPTeC).

Appendix A: Closed-Form Expression for v_3

$$\begin{aligned}
v_3 = & \mp \frac{[\dot{\omega} \times (\omega \times \dot{\omega}) + \omega \times (\omega \times \ddot{\omega})] \cdot \{\|\omega\|^2 \cdot (\dot{\omega} \times v + \omega \times \ddot{v}) - 2\omega \cdot \dot{\omega} \cdot (\omega \times v)\}}{\|\omega\|^3 \cdot \|\omega \times \dot{\omega}\|^2} \\
& \mp \frac{(\omega \times (\omega \times \dot{\omega})) \cdot \{\|\omega\|^2 \cdot (\dot{\omega} \times v + 2\dot{\omega} \times \dot{v} + \omega \times \ddot{v}) - 2(\|\dot{\omega}\|^2 + \omega \cdot \dot{\omega})(\omega \times v)\}}{\|\omega\|^3 \cdot \|\omega \times \dot{\omega}\|^2} \\
& \pm \left[\frac{3}{2} \cdot \frac{\omega \cdot \dot{\omega}}{\|\omega\|^2} + \frac{(\omega \cdot \times \dot{\omega}) \cdot (\omega \times \dot{\omega})}{\|\omega \times \dot{\omega}\|^2} \right] \cdot \frac{(\omega \times (\omega \times \dot{\omega})) \cdot \{\|\omega\|^2 \cdot (\dot{\omega} \times v - \omega \times \ddot{v}) - 2(\omega \cdot \dot{\omega})(\omega \times v)\}}{\|\omega\|^3 \cdot \|\omega \times \dot{\omega}\|^2} \quad (A1)
\end{aligned}$$

Appendix B: Proof of Invariance of v_2 and v_3

To verify the invariance of v_2 we have to look at how Eq. (23) changes if v is replaced by v^* with $v^* - v = u \times \omega$. Apart from division by a constant $\|\omega \times \dot{\omega}\| \cdot \|\omega\|^4$ this change corresponds to

$$\Delta = (\omega \times \dot{\omega}) \cdot [\Delta_1 + \Delta_2 + \Delta_3] \quad (B1)$$

where

$$\Delta_1 = \dot{\omega} \times (u \times \omega) \cdot \|\omega\|^2 \quad (B2)$$

$$\Delta_2 = \omega \times (u \times \dot{\omega}) \cdot \|\omega\|^2 \quad (B3)$$

$$\Delta_3 = -2\omega \times (u \times \omega) \cdot (\omega \dot{\omega}) \quad (B4)$$

Using the property $a \times (b \times c) = b(a \cdot c) - c(a \cdot b)$, each of the three terms between the square brackets is reworked as:

$$\Delta_1 = u(\dot{\omega} \cdot \omega)(\omega \cdot \omega) - \omega(\dot{\omega} \cdot u)(\omega \cdot \omega)$$

$$\Delta_2 = u(\dot{\omega} \cdot \omega)(\omega \cdot \omega) - \dot{\omega}(\omega \cdot u)(\omega \cdot \omega)$$

$$\Delta_3 = -2u(\dot{\omega} \cdot \omega)(\omega \cdot \omega) + 2\omega(\omega \cdot u)(\omega \cdot \dot{\omega})$$

While in the above expressions the first terms on the right hand side add to zero, each of the second terms is perpendicular to

$(\omega \times \dot{\omega})$, since $a \cdot (a \times b) = 0$. Hence Δ will be zero.

The proof of invariance for v_3 proceeds along the same lines, starting from the closed-form expression of v_3 .

References

- [1] Black, M., and Jepson, A., 1998, "A Probabilistic Framework for Matching Temporal Trajectories: Condensation-Based Recognition of Gestures and Expressions," *Proceedings of the European Conference on Computer Vision (ECCV)*, Springer-Verlag, Freiburg, Germany, pp. 900-924.
- [2] Rao, C., Yilmaz, A., and Shah, M., 2002, "View-Invariant Representation and Recognition of Actions," *Int. J. Comput. Vis.*, **50**(2), pp. 203-226.
- [3] Psarrou, A., Gong, S., and Walter, M., 2002, "Recognition of Human Gestures and Behaviour Based on Motion Trajectories," *Image Vis. Comput.*, **20**, pp. 349-358.
- [4] Yamada, Y., Umetani, Y., Daitoh, H., and Sakai, T., 1999, "Construction of a Human/Robot Coexistence System Based on a Model of Human Will—Intention and Desire," *International Conference on Robotics and Automation*, Detroit, MI, pp. 2861-2867.
- [5] Aleotti, J., and Caselli, S., 2005, "Trajectory Clustering and Stochastic Approximation for Robot Programming by Demonstration," *Proceedings of the IEEE/RSJ International Conference on Intelligent Robots and Systems*, Edmonton, Canada, pp. 1029-1034.
- [6] Friedrich, H., Münch, S., and Dillmann, R., 1996, "Robot Programming by Demonstration (RPD): Supporting the Induction by Human Interaction," *Mach. Learn.*, **23**, pp. 163-189.
- [7] Frenet, F., 1847, "Sur les courbes à courbure," Ph.D. thesis, Toulouse, France.
- [8] Wu, S., and Li, Y., 2008, "On Signature Invariants for Effective Motion Tra-

- jectory Recognition," *Int. J. Robot. Res.*, **27**(8), pp. 895–917.
- [9] Chasles, M., 1830, "Note sur les propriétés générales du système de deux corps semblables entr'eux et placés d'une manière quelconque dans l'espace; et sur le déplacement fini ou in finiment petit d'un corps solide libre," *Bulletin des Sciences Mathématiques, Astronomiques, Physiques et Chimiques*, **14**, pp. 321–326.
- [10] Ceccarelli, M., 1995, "Screw Axis Defined by Giulio Mozzi in 1763," Ninth World Congress IFToMM, Milano, Italy, pp. 3187–3190.
- [11] Mozzi, G., 1763, "Discorso Matematico sopra il Rotamento Momentaneo dei Corpi," Stamperia del Donato Campo, Napoli.
- [12] Skreiner, M., 1966, "A Study of the Geometry and the Kinematics of Instantaneous Spatial Motion," *J. Mech.*, **1**, pp. 115–143.
- [13] Veldkamp, G. R., 1969, "Acceleration Axes and Acceleration Distribution in Spatial Motion," *ASME J. Eng. Ind.*, **91**, pp. 147–151.
- [14] Skreiner, M., 1969, "Discussion on "Acceleration Axes and Acceleration Distribution in Spatial Motion"," *ASME J. Eng. Ind.*, **13**, pp. 150–151.
- [15] Bokelberg, E. H., Hunt, K. H., and Ridley, P. R., 1992, "Spatial Motion—I. Points of Inflection and the Differential Geometry of Screws," *Mech. Mach. Theory*, **27**(1), pp. 1–15.
- [16] Phillips, J., and Hunt, K., 1964, "On the Theorem of Three Axes in the Spatial Motion of Three Bodies," *J. Appl. Sci.*, **15**(4), pp. 267–287.
- [17] Angeles, J., 1986, "Automatic Computation of the Screw Parameters of Rigid-Body Motions. Part II: Infinitesimally-Separated Positions," *ASME J. Dyn. Syst., Meas., Control*, **108**, pp. 39–43.
- [18] Angeles, J., 1987, "Computation of Rigid-Body Angular Acceleration From Point-Acceleration Measurements," *ASME J. Dyn. Syst., Meas., Control*, pp. 124–127.
- [19] Angeles, J., 1988, *Rational Kinematics*, Springer, New York.
- [20] Sommer, H. J., III, 1992, "Determination of First and Second Order Instant Screw Parameters From Landmark Trajectories," *ASME J. Mech. Des.*, **114**, pp. 274–282.
- [21] Page, A., 2009, "Experimental Analysis of Rigid Body Motion. A Vector Method to Determine Finite and Infinitesimal Displacements From Point Coordinates," *ASME J. Mech. Des.*, **131**, p. 031005.
- [22] Fenton, R. G., and Willgoss, R. A., 1990, "Comparison of Methods for Determining Screw Parameters of Infinitesimal Rigid Body Motion From Position and Velocity Data," *ASME J. Dyn. Syst., Meas., Control*, **112**, pp. 711–716.
- [23] Veldkamp, G. R., 1967, "Canonical Systems and Instantaneous Invariants in Spatial Kinematics," *J. Mech.*, **2**, pp. 329–333.
- [24] Bottema, O., and Roth, B., 1979, *Theoretical Kinematics* (Series in Applied Mathematics and Mechanics), Vol. 24, North-Holland, Amsterdam, the Netherlands.
- [25] Roth, B., 2005, "Finding Geometric Invariants From Time-Based Invariants for Spherical and Spatial Motions," *ASME J. Mech. Des.*, **127**, pp. 227–231.
- [26] Kirson, Y., and Yang, A., 1978, "Instantaneous Invariants of Three-Dimensional Kinematics," *ASME J. Appl. Mech.*, **45**, pp. 409–414.
- [27] McCarthy, J., and Roth, B., 1982, "Instantaneous Properties of trajectories Generated by Planar, Spherical, and Spatial Rigid Body Motions," *ASME J. Mech. Des.*, **104**, pp. 39–51.
- [28] McCarthy, J., and Ravani, B., 1986, "Differential Kinematics of Spherical and Spatial Motions Using Kinematic Mapping," *ASME J. Appl. Mech.*, **53**, pp. 15–22.
- [29] Lee, C., Yang, A., and Ravani, B., 1993, "Coordinate System Independent Form of Instantaneous Invariants in Spatial Kinematics," *ASME J. Mech. Des.*, **115**, pp. 946–952.
- [30] Stachel, H., 2000, "Instantaneous Spatial Kinematics and the Invariants of the Axodes," *Proceedings of the Ball 2000 Symposium*, Cambridge University Press, London, pp. 1–14.
- [31] Denavit, J., and Hartenberg, R. S., 1955, "A Kinematic Notation for Lower-Pair Mechanisms Based on Matrices," *ASME J. Appl. Mech.*, **23**, pp. 215–221.
- [32] Skreiner, M., 1967, "On the Points of Inflection in General Spatial Motion," *J. Mech.*, **2**, pp. 429–433.
- [33] Paul, R. P., 1981, *Robot Manipulators: Mathematics, Programming, and Control*, MIT, Cambridge, MA.